AIAA SciTech Forum
7-11 January 2019, San Diego, Califo
AIAA Scitech 2019 Forum

10.2514/6.2019-0731

SAND2019-1981C

Multi-Scalar Measurements of Premixed Flames in Extreme Turbulence Using Raman/Rayleigh Diagnostics

Timothy M. Wabel[1]
University of Toronto, Toronto, ON, M3H 5M6, Canada

Adam M. Steinberg[2]
Georgia Institute of Technology, Atlanta, GA, 30332, USA

and
Robert S. Barlow[3]
Sandia National Laboratories, Livermore, CA, 94550, USA

This work reports simultaneous multi-scalar measurements of a high Karlovitz number lean-premixed methane/air Bunsen flame surrounded by a large vitiated co-flow. Flames in this burner (the Hi-Pilot burner) have previously been analyzed in the context of perfectly premixed combustion. Radial profiles of simultaneous Raman/Rayleigh scattering were recorded at multiple downstream locations throughout the flame brush at a jet exit Karlovitz number of $Ka_{T,P} = 4 \times 10^2$. The multi-scalar measurements reported here indicate that the reaction zones cannot be considered perfectly premixed at the equivalence ratio of the jet. Instead, mixing occurs between the pilot and main reactants prior to burning, such that the reaction layers are primarily stratified. The local equivalence ratio at the reaction surface attains an intermediate value between the two streams. The measurements show that the composition of the reactants at the flame front vary downstream, with heat release near the jet exit occurring at equivalence ratios similar to that of the pilot, while heat release at downstream locations occurs at equivalence ratios that are closer to that of the central jet. Mass fractions of CO, evaluated from the Raman scattering, do not show evidence of extinction at any locations in the jet. Based on these results, the specific mechanism causing stratification cannot yet be identified. The implications of these findings for the regime diagram as well as previous measurements of high $Ka_{T,P}$ flames are discussed.

I. Nomenclature

u'	=	root-mean-square of velocity fluctuations
L	=	integral length scale
ν	=	kinematic viscosity
ρ	=	density
S_L	=	unstretched laminar flame speed
D^*	=	characteristic diffusivity of the reactants computed at the temperature of the reaction surface
τ_{η^*}	=	Kolmogorov time scale of turbulence, computed at the temperature of the reaction surface
$\delta_{F,L}$	=	laminar flame thickness
$\delta_{F,L,P}$	=	laminar flame thickness as defined by Peters [2], D^*/S_L
$Ka_{T,P}$	=	turbulent Karlovitz number as defined by Peters [2], $\left(\frac{u'}{S_L}\right)^{\frac{3}{2}}\left(\frac{\delta_{F,L,P}}{L}\right)^{\frac{1}{2}}$
Re_T	=	turbulent Reynolds number, $u'L/\nu$
ϕ	=	equivalence ratio
X_i	=	mole fraction of species *i*

[1] Post-Doctoral Research Fellow, Institute for Aerospace Studies, AIAA Member
[2] Associate Professor, School of Aerospace Engineering, AIAA Associate Fellow
[3] Distinguished Member of Technical Staff, Reacting Flow Research Department, AIAA Senior Member

Y_i = mass fraction of species i
w_i = molar mass of species i

II. Introduction

Realistic combustion devices operate with highly turbulent flows, and the effect of this turbulence on the heat release field is not yet fully understood [1]. It has been predicted that when the time scales of the turbulent flow become small enough relative to those of the chemical reactions of the inner layer of the flame, reaction layers can be disrupted or broadened [2]. This criterion has been expressed mathematically by Peters in terms of the turbulent Karlovitz number ($Ka_{T,P}$) as [2-3]:

$$Ka_{T,P} = \frac{\tau_F}{\tau_{\eta^*}} = \frac{\delta_{F,L,P}/S_L}{\tau_{\eta^*}} = \left(\frac{u'}{S_L}\right)^{\frac{3}{2}} \left(\frac{\delta_{F,L,P}}{L}\right)^{1/2} \quad (1)$$

where $\delta_{F,L,P}$ is the laminar flame thickness as defined by Peters [2], D^*/S_L. D^* is the diffusivity, S_L is the unstretched laminar flame speed, L is the integral length scale, u' is the root-mean-square of velocity fluctuations, and τ_{η^*} is the Kolmogorov time scale. In Eq. 1, D^* and τ_{η^*} are evaluated at the reaction layer temperature (typically near 1500 K). The value of $Ka_{T,P}$ therefore is explicitly related to the relative time scales of the turbulence and flame chemistry, and this reasoning has been used to formulate boundaries for regimes of turbulent premixed combustion [2-3]. Conventional regime diagrams assume the reaction layer is approximately ten times thinner than the laminar flame thickness, resulting in a boundary of $Ka_{T,P} = 100$ beyond which broadened, broken, or distributed reactions should occur.

It has been a goal of the combustion community for some time to validate this proposed boundary and identify changes in reaction layer structure with increasing $Ka_{T,P}$. Evidence of reaction layer broadening has been seen in several direct numerical simulations (DNS) and some experiments. Aspden et al. [4] simulated a high-Karlovitz number supernovae flame and observed distributed reactions for the first time. In experiments, Raman and/or Rayleigh scattering has been used to indicate broadening of the flame brush in piloted premixed jet flames by Chen et al. [5], Mansour et al. [6], and Dunn et al. [7-9]. However, none of these studies found evidence of distributed reaction zones.

Experimental data showing distributed reactions using planar laser diagnostics were first observed in a high Karlovitz number jet flame by Zhou et al. [10]. They achieved Karlovitz numbers exceeding 1,000 at the jet exit by utilizing a small-diameter, large velocity jet and extremely lean methane-air mixtures ($\phi_{jet} = 0.4$). Reaction layers were visualized using planar laser-induced fluorescence (PLIF) of the HCO and CH radicals, and distributed reactions were observed, with relatively homogenous CH and HCO-PLIF throughout the downstream regions of the jet.

However, recent DNS simulations of this flame [11] have indicated that the heat release does not occur at the equivalence ratio of the main reactants. Instead, prior to combustion, some mixing occurs between the central jet and the richer combustion products from the pilot ($\phi_{pilot} = 0.9$), and the reaction layers are therefore primarily stratified in this configuration. The mechanism producing this mixing was not explicitly identified. However, it was shown that the magnitude of heat release rate near the jet exit (where strain rates and $Ka_{T,P}$ were the highest) was reduced, indicating partial extinction or weakening of the reaction layers. However, the heat release rate was not observed to drop to zero at any locations in the flame. These results suggest that mixing across the flame zone may be possible, even in the absence of total extinction of the reaction layer, if the mixing rates are large enough relative to the flame chemistry.

In the Hi-Pilot burner, a large diameter Bunsen burner, the planar spatial distribution of CH_2O, OH, and CH were recorded using PLIF across a wide range of turbulence conditions [3,12]. The reaction layers, indicated by the spatial overlap of OH and CH_2O-PLIF and by the CH-PLIF signals, remained at or near the laminar thickness even at extreme levels of turbulence ($Ka_{T,P} > 500$). However, the preheat zone upstream of the reaction layers was significantly broadened [3,12]. For many run conditions in the Hi-Pilot burner, the preheat zone was broadened to entirely fill the reactants in the jet core [13]. Thus, although the chemistry of the inner layer of the reaction zone was not visually disrupted, the turbulence had a significant effect on global flame properties through preheat broadening, possibly due to enhanced turbulent diffusivity. It is expected that this should lead to an increased chemical reaction rate relative to

the laminar value. This hypothesis was also supported by measurements of the global consumption speed [13] (a measure of the total rate at which reactants are consumed), which was greater than could be explained by the measured increase in flame surface area due to turbulent wrinkling. To reconcile these two observations, it was presumed that the local consumption rate of reactants per unit flame surface area (and thus the heat release rate) must be enhanced. This hypothesis was supported by the local flame speed measurements of Osborne et al. [14].

Multi-scalar measurements of flame species and temperature are an important step for improved understanding of turbulence-chemistry interactions in highly turbulent flames and can provide crucial data to help address the questions raised above [15-16]. Furthermore, these data are necessary to further develop and validate combustion models, which are a requirement to accurately simulate realistic combustion devices [17]. The present work applies simultaneous line Raman and Rayleigh measurements in the Hi-Pilot burner to determine the temperature and seven major species concentrations (N_2, O_2, CO, CO_2, CH_4, H_2, and H_2O). The primary goal of this paper is to apply the multi-scalar laser diagnostics in a high-$Ka_{T,P}$ flame to identify the effect of turbulence on the reactant's chemical composition and the detailed structure of the flame.

III. Experimental Procedure

Experiments were conducted in the Hi-Pilot burner, which is illustrated in Fig. 1 and has been characterized in several previous studies [3,12-13]. The Hi-Pilot is a Bunsen burner with a large (108 mm) diameter co-flow surrounding a 21.6 mm central jet. The jet has a converging-diverging nozzle to prevent flashback, and turbulence is generated using slotted plates placed upstream of the contraction section. Impinging jets have been used in previous experiments to increase the turbulence levels but are not used in the present measurements.

One run condition is studied in this work, the parameters of which are listed in Table 1 below. The air mass flow rates selected for this study correspond to Case 4B from previous measurements in the Hi-Pilot [3,12-13]. The equivalence ratio of the main reactants issuing from the central jet was $\phi_{jet} = 0.65$. A richer co-flow pilot of $\phi_{pilot} = 0.9$ was used in this work. Previous Hi-Pilot cases with a lean central jet have also used a richer co-flow [3]. The pilot was run at a larger equivalence ratio so that any potential entrainment of pilot combustion products could be identified with the multi-scalar diagnostics. The turbulent Karlovitz number at this run condition was $Ka_{T,P} = 4 \times 10^2$, which is above the theoretical broken/distributed reaction zones boundary predicted by Peters [2]. Previous PLIF measurements in the Hi-Pilot showed that flames in these turbulence conditions possess broadened preheat zones, but that the spatial extent of the inner reaction layer is not significantly perturbed [3,12].

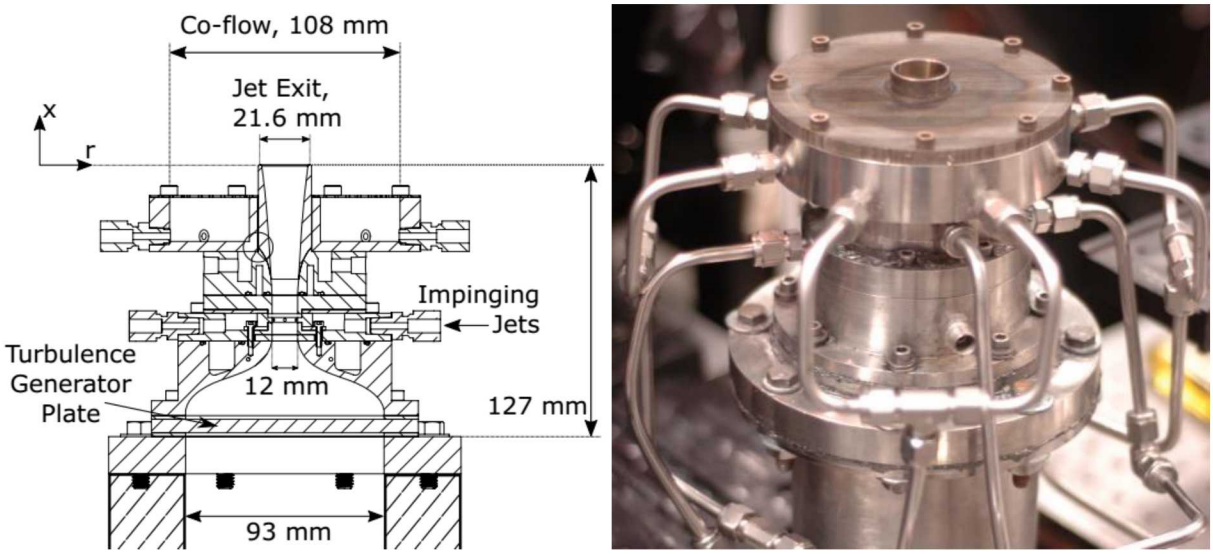

Figure 1: The Hi-Pilot burner.

Table 1: Run conditions for the combined Raman/Rayleigh/LIF measurements

Case	ϕ_{jet}	ϕ_{pilot}	Main jet reactants (g/s)	Pilot reactants (g/s)	u'/S_L	$Ka_{T,P}$
4B-0.65	0.65	0.9	13.67	9.47	139	4×10^2

Data were collected at multiple downstream locations, and in this paper, we present results from $x = 10, 20, 40$ and 60 mm. Radial profiles were measured throughout the flame zone, extending into the co-flow until no more reaction layers were observed. Similarly, downstream profiles were continued until reactants were no longer observed in the OH-PLIF and Raman data.

The experimental configuration is illustrated in Fig. 2 below. The Raman/Rayleigh probe volume was provided by four frequency doubled Nd:YAG lasers that were optically stretched and combined in sequence to produce a 1.4 J/pulse beam with a duration of approximately 400 ns and beam diameter of approximately 220 μm. Measurements of CO-LIF and crossed-plane OH-PLIF were also performed and will be presented in a future publication.

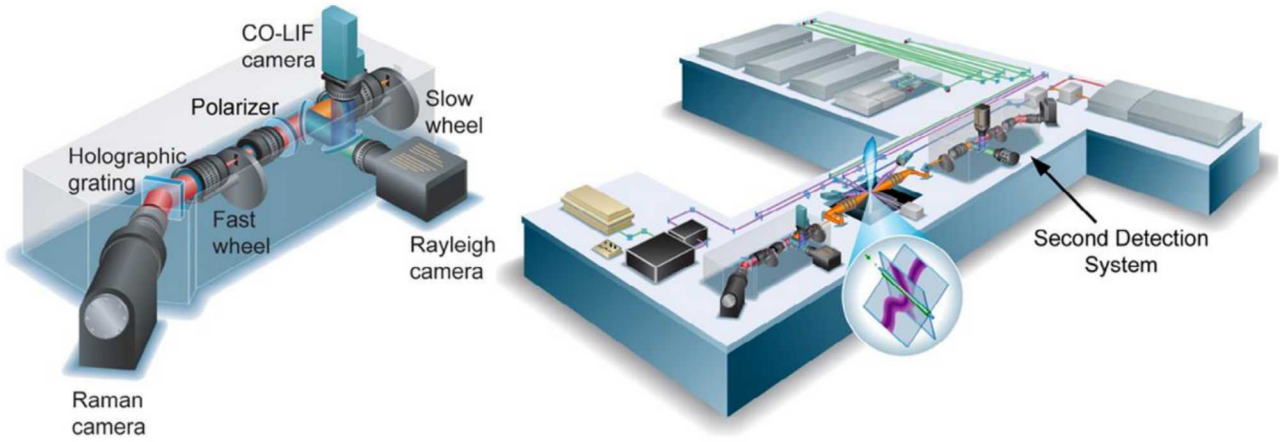

Figure 2: Experimental Setup of the Raman/Rayleigh/PLIF diagnostics. The second detection system was not used in this study. The LIF/PLIF measurements are not reported in this paper but will be included in a future publication.

Two 150 mm Linos Photonics lenses (set to f/2 and f/4, respectively) were used to focus the Raman/Rayleigh signal onto the detection system. The exposure time of the cameras was controlled via a pair of rotating wheels with narrow slits designed to pass light once per revolution (see Fig. 2). The slower rotating wheel was placed in front of both the Raman and Rayleigh cameras, producing a 300 μs gate time. This was the gate time for the Rayleigh camera. The second, faster rotating wheel was placed in front of the Raman camera producing a gate time of 3.9 μs.

A custom transmission grating (1200 lines/mm) and mirrors/filters were used to separate the Rayleigh scattering at 532 nm from the Raman signal (~550 – 700 nm) and CO fluorescence (~480 – 488 nm). The Rayleigh signal was measured with a Princeton Instruments 1340/400 EMB CCD camera. Raman scattering was detected using a non-intensified, low-noise, cryogenically cooled CCD camera (Princeton Instruments VersArray 1300 B with CryoTiger cooling unit, operating at -100 C).

Combined Raman/Rayleigh measurements were acquired with a data spacing of 20 μm along the 6-mm probe volume, and a method of wavelet adaptive thresholding and reconstruction (WATR) [18] was applied to each 1D channel to reduce noise. The Raman/Rayleigh data were then processed using the hybrid approach described by Fuest et al. [15]. The hybrid approach mitigates the detrimental effects of beam steering that occurs in turbulent flames as well as optical distortion ("bowing") of the image as it passes through the entrance slit to the spectrometer.

The local equivalence ratio, ϕ, was defined following Sweeney et al. [19] as:

$$\phi = \frac{X_{CO_2}+2X_{CH_4}+X_{CO}+0.5(X_{H_2O}+X_{H_2})}{X_{CO_2}+X_{O_2}+0.5(X_{H_2O}+X_{CO})} \quad (2)$$

where X_i is the mole fraction of the ith species. Thus, ϕ represents the local equivalence ratio defined using the instantaneous, local fuel/oxygen atom balance obtained from the measured Raman species concentrations. It is similar to the normalized Bilger mixture fraction [19-20], and is equal to the equivalence ratio of either the main reactants or co-flow combustion products when far from the flame surface. In a one dimensional, laminar premixed flame ϕ will be approximately constant at all locations (although differential diffusion affects will slightly perturb ϕ near the areas of heat release, particularly for rich flames [21]).

The local progress variable of the flame was also evaluated. A new definition of the progress variable was recently proposed by Barlow et al. [22], which is computed from the measured species mass fractions as:

$$c_O = \frac{Y_{CO_2}\left(\frac{w_{O_2}}{w_{CO_2}}\right)+Y_{CO}\left(\frac{w_O}{w_{CO}}\right)+Y_{H_2O}\left(\frac{w_O}{w_{H_2O}}\right)}{\left(Y_{CO_2}\left(\frac{w_{O_2}}{w_{CO_2}}\right)+Y_{CO}\left(\frac{w_{O_2}}{w_{CO}}\right)+Y_{H_2O}\left(\frac{w_O}{w_{H_2O}}\right)+Y_{H_2}\left(\frac{w_O}{w_{H_2}}\right)+Y_{CH_4}\left(\frac{2w_{O_2}}{w_{CH_4}}\right)\right)}; \quad \phi < 1 \tag{3}$$

In Eq. 3, Y_i and w_i correspond to the mass fraction and molar mass of the ith species, respectively. The definition of c_O given in Eq. 3 is essentially the mass of oxygen bound in the products CO_2, CO and H_2O divided by the mass of oxygen that would be bound if the gas mixture were in the fully-burnt state. This formulation was shown in Ref. [22] to have some advantages over other definitions of the progress variable. It can be easily computed from the multi-scalar measurements conducted here and can also be easily extracted from a simulation dataset.

IV. Results

Scatter plots of the local equivalence ratio ϕ versus temperature at nine locations in the Hi-Pilot are presented in Fig. 3. Near the jet exit (x = 10, 20 mm), a strong positive correlation exists between ϕ and temperature at all radial locations. At these upstream locations, no high temperature ϕ = 0.65 samples are observed, indicating that reactants do not burn at the equivalence ratio of the fluid issuing from the central jet. High temperature samples at equivalence ratios approximately corresponding to the jet are only observed at downstream locations, e.g. $x = 60$ mm.

The results in Fig. 3 indicate significant turbulent mixing of the jet and co-flow fluid at upstream locations. Therefore, it is important to consider whether this mixing occurs through regions of completely extinguished reactions or whether burning is occurring simultaneously to the mixing of co-flow and jet fluids. Figure 4 presents scatter plots of the mass fraction of CO (Y_{CO}, derived from the Raman scattering measurements) versus temperature colored by equivalence ratio. CO is produced and rapidly consumed near the primary reaction zone of a premixed flame, and therefore the peak Y_{CO} indicates the location of heat release [18,23-24]. Due to its proximity to the reaction layer, Y_{CO} reaches a maximum at intermediate temperatures in a premixed flame (around 1500 K for the present run conditions) [25]. Non-reacting mixing between the reactants and products (i.e. extinction) would correspond to a straight line between the low- and high-temperature states. Figure 4 shows that local maxima in Y_{CO} occur near 1500 K for all locations in Hi-Pilot, indicating the presence of reaction zones. Extinction is observed rarely in the present data. Therefore, the multi-scalar measurements do not show evidence of non-reacting mixing between the co-flow products and main reactants at any locations in the jet. However, the measurements reported here were not made below $x = 10$ mm, and thus the possibility of extinction upstream of this location cannot be assessed from the present data set.

Regardless, the equivalence ratio at the location of maximum Y_{CO} does not correspond to that of the reactants issuing from the central jet. The present Hi-Pilot run condition is therefore classified as a stratified flame. This is an important result, as interpretation of results from previous Hi-Pilot cases has been done in the context of perfectly premixed flames. Some potential implications of this finding are discussed in Section **V**.

It is interesting to note that the gradient of ϕ in temperature space is smaller as the flow evolves downstream. At $x = 10$ or 20 mm, particularly near the jet centerline, there is a nearly linear correlation between the two variables. However, the local equivalence ratio changes much more gradually at $x = 60$ mm, indicating a more uniform reactant composition throughout the preheat zone. Nonetheless, the reaction zones at these downstream locations are still primarily stratified and there are few samples of high-temperature $\phi = 0.65$ products.

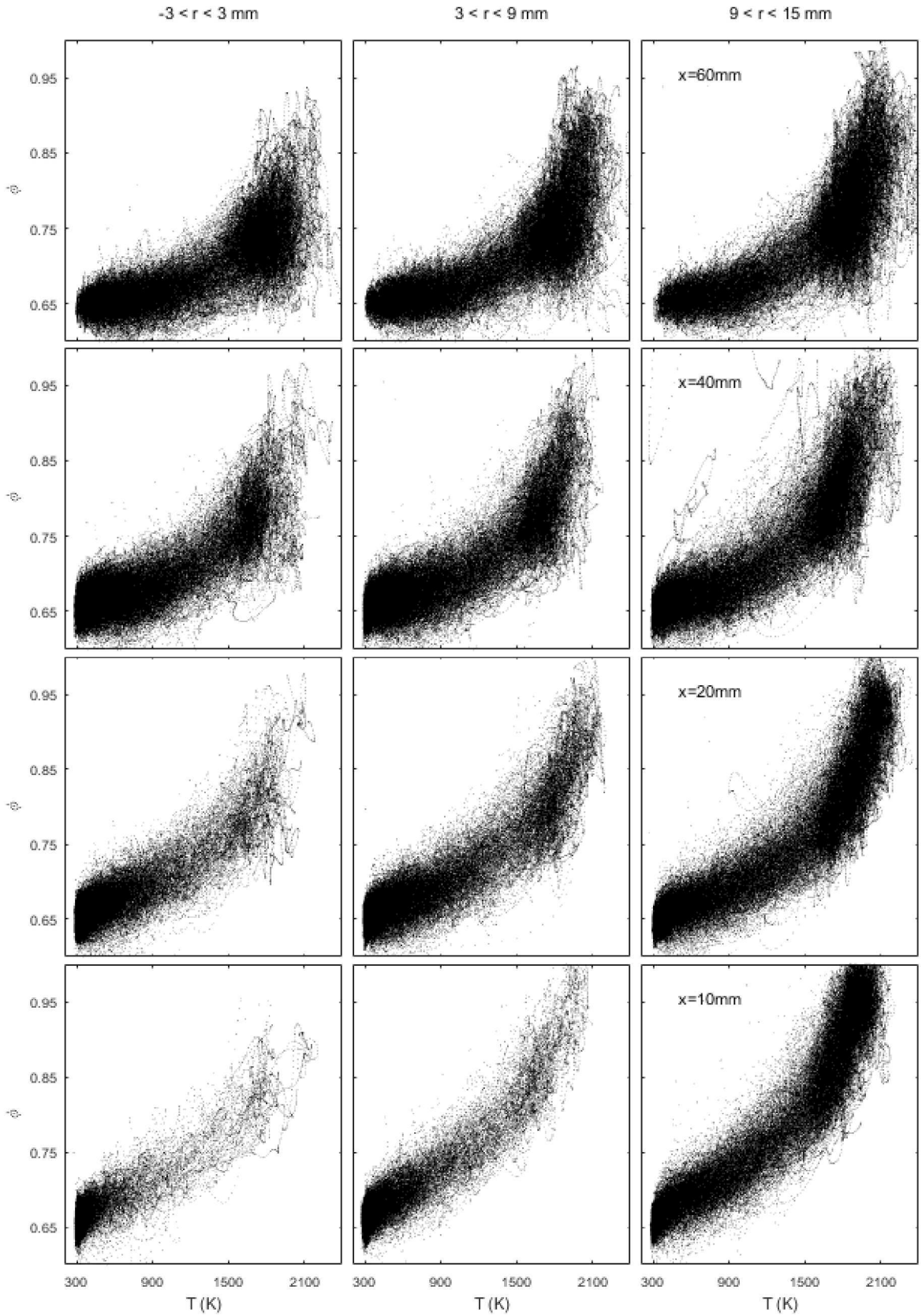

Figure 3. Scatter plots of ϕ versus temperature for 12 locations in the Hi-Pilot burner. The figure indicates stratified combustion, as almost no high temperature samples of $\phi = 0.65$ are observed.

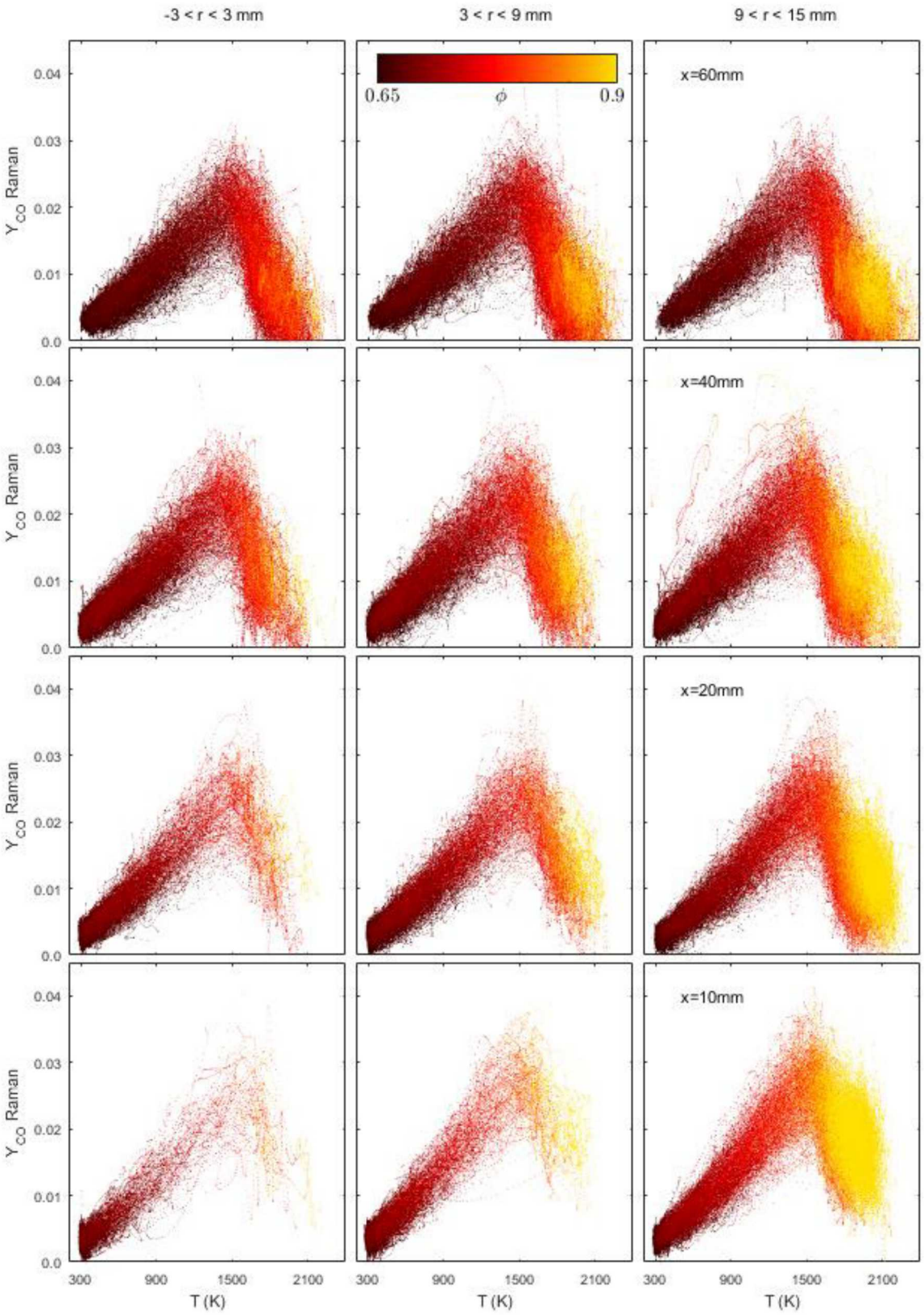

Figure 4. Scatter plots of CO mass fraction (Y_{CO}) versus temperature for 12 locations in the Hi-Pilot burner. Color map corresponds to ϕ. The figure indicates reaction zones are present at all locations, as a peak at intermediate temperatures is always present.

Figure 5 shows probability density functions of ϕ conditioned on the region of peak heat release (defined here as $0.7 < c_0 < 0.8$) for the Hi-Pilot flame. The figure reports ensemble statistics computed from all radial locations measured for a given downstream value of x. The dashed lines indicate the composition of the main reactants, $\phi_{jet} = 0.65$. Figure 5 shows that the most probable ϕ in the vicinity of the reaction zone is always greater than ϕ_{jet}, which is further evidence of the stratified reaction zones present for this run condition. It is interesting to observe that there is a shift in the composition of the reactants near the reaction layer as the flow evolves downstream. Near the jet exit, heat release occurs at $\phi \approx 0.78$, which is closer to the composition of the co-flow combustion products ($\phi_{pilot} = 0.9$). However, at downstream locations, the heat release occurs at values of ϕ closer to the main reactants, with a maximum near $\phi \approx 0.72$. A similar trend was observed in recent DNS by Wang et al. in a high-Ka_T jet flame [9]. This may be due to decreased mixing rates with decreasing turbulence intensity at farther downstream locations.

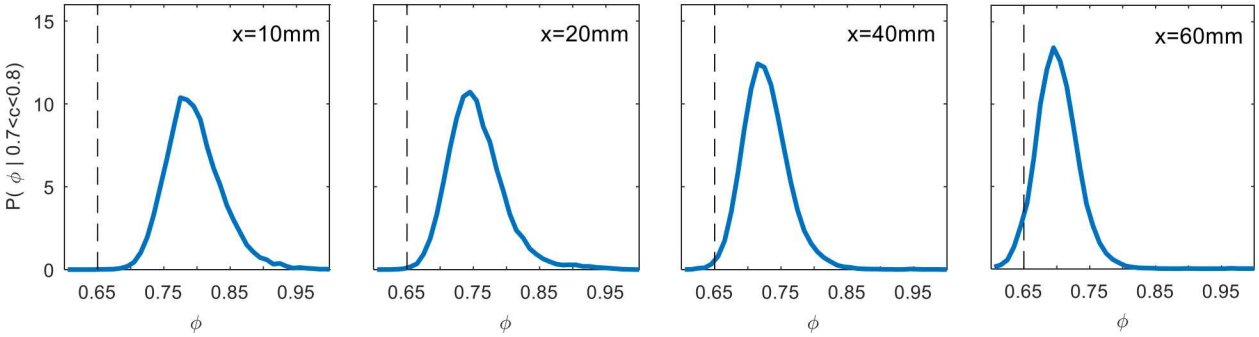

Figure 5. Probability density functions of ϕ conditional on progress variable $0.7 < c_0 < 0.8$ for the Hi-Pilot flame.

V. Discussion

The results of Figs. 3-5 indicate that the present Hi-Pilot run condition is not a perfectly premixed flame. Instead, it is a stratified flame with a significant gradient in ϕ in temperature-space, particularly at upstream positions. It is important that the mechanism producing stratification be identified. The Raman scattering measurements alone cannot reveal the means by which mixing occurs in the Hi-Pilot burner. However, we can hypothesize several possibilities.

The variation of ϕ conditioned on the location of maximum heat release rate (Fig. 5) displays many simlarities to the DNS results of Wang et al. in a high-$Ka_{T,P}$ jet flame [9]. Their simulations showed reduced heat release rates for $x/D < 10$, allowing co-flow combustion products to mix with the main reactants in this region. Total extinction of the reaction layers was not observed. However, the species gradients induced by turbulent advection were sufficient to produce mixing across the flame zone. It may be that a similar mechanism is occurring in the Hi-Pilot burner due to the very large $Ka_{T,P}$ near the exit plane (with $\tau_{\eta^*} \ll \tau_f$, from Eq. 1).

Another plausible explanation is complete extinction of the reaction layers in these upstream regions, leading to non-reacting mixing between the two streams. It is noted that no previous planar flame structure measurements in the Hi-Pilot burner have reported any significant degree of extinction [3,10], nor do the CO mass fraction profiles shown in Fig. 4. Instead, reaction layers of approximately the laminar thickness have been measured at all positions in the flame, in agreement with the present multi-scalar diagnostics. However, all of these data have been restricted to $x > 5$ mm downstream of the exit plane. It is possible that extinction is occurring upstream of this location, and requires further experimental investigation.

Finally, a third possible mechanism producing stratification is intermittent separation of the central jet from the diverging portion of the nozzle. Such separation could reconcile the observation of stratified reaction zones with the lack of visible extinction in these as well as previous data. A separating flow might allow the flame to propagate briefly over the centerline, pulling combustion products from the pilot into the core of the jet. This would allow mixing between the two streams before the flame returns to its anchored position on the burner nozzle.

The multi-scalar measurements suggest that it is problematic to place the present Hi-Pilot run condition on a premixed combustion regime diagram. All Hi-Pilot run conditions that have previously been placed on a regime diagram have used a co-flow of different composition from the main reactants. Therefore, it is important to identify

which of these run conditions possess stratified reaction layers. For those cases, they may need to be removed from the regime diagram, as they do not pertain to perfectly premixed combustion.

Depending on the particular mechanism producing stratification in the Hi-Pilot, there may be different implications for a regime diagram. If it is due simply to extinction or significant reaction layer weakening near the jet exit (where the strain rates are the largest), then the conclusion may be that these flames exceed a critical $Ka_{T,P}$ at these locations. In jet and Bunsen configurations, high $Ka_{T,P}$ are typically achieved by a combination of high jet velocities and small laminar flame speeds; it therefore may not be surprising that these conditions can disrupt the flame chemistry near the jet exit. However, if extinction is occurring, then these regions of the flame may be appropriately placed in the broken reaction layers regime, as they meet the criteria established by Peters [2]. This would be contrary to the findings of previous studies [3,10] that observed thin reaction layers at all turbulence conditions. However, they did not measure upstream regions near the exit plane ($x < 5$ mm), and were not using multi-scalar diagnostics that would be capable of detecting mixing.

It is also possible that mixing of co-flow combustion products with the main reactants can explain why thin reaction zones were observed at such large $Ka_{T,P}$ in downstream locations in previous studies [3]. As shown in [3], thin and continuous reaction layers have been observed in the Hi-Pilot for $Ka_{T,P} > 500$. However, the present results suggest that the laminar thermo-chemical properties that were used to compute $Ka_{T,P}$ in downstream locations may be incorrect, as $S_L, \delta_{F,L}$, etc. will differ substantially after mixing occurrs. If the true thermochemical properties of the reactants at the region of heat release could be used to estimate $Ka_{T,P}$ at the flame front, it may be found that the reaction layers obey the predictions of [2] more closely than was found in [3].

VI. Conclusion

Combined Raman/Rayleigh diagnostics have been applied in the Hi-Pilot burner for the first time. The multi-scalar measurements of the lean-premixed methane/air flames were made in the range of extreme turbulence with centerline jet-exit conditions of $Ka_{T,P} = 422$ and $u'/S_L = 139$. The main reactants were run at lean conditions, $\phi_{jet} = 0.6$, while the surrounding co-flow pilot was run at a richer equivalence ratio of $\phi_{pilot} = 0.9$. These flames were known to lie in the broadened preheat – thin reaction zones regime based on previous flame structure measurements. The conclusions are as follows:

1) The multi-scalar measurements show that the present run conditions depart from perfectly premixed combustion. Instead, mixing occurs between the pilot gases and the main reactants prior to burning, and the local equivalence ratio at the reaction surface attains an intermediate value between that of the two streams. Therefore, the reaction layers in this Hi-Pilot run condition are primarily stratified rather than premixed.
2) The measurements show that the composition of the reactants at the flame front vary as the flow evolves downstream. Near the exit plane, heat release occurs at equivalence ratios nearer to that of the pilot. In downstream locations, the composition near the heat release layers trends towards that of the main reactants, ϕ_{jet}.
3) CO mass fractions do not show evidence of extinction, and reaction zones are measured at all locations throughout the jet. The mechanism causing stratification cannot be identified from the multi-scalar diagnostics, but it is possible that mixing is occurring across the flame brush due to finite-rate chemistry.
4) The measurements have potential implications for the regime diagram predicted by Peters [2], and it is possible that run conditions previously thought to have a broadened preheat – thin reaction zone structure are in fact located in the broken reaction zones regime. These observations are preliminary and require further experimental investigation.

Acknowledgements

T. Wabel and A. Steinberg were supported by the US Air Force Office of Scientific Research under Grant FA9550-17, Project Monitor Dr. Chiping Li. R. Barlow was supported by the U.S. Department of Energy, Office of Basic Energy Sciences, Division of Chemical Sciences, Geosciences, and Biosciences. Sandia National Laboratories is a multi-mission laboratory managed and operated by National Technology and Engineering Solutions of Sandia, LLC., a wholly owned subsidiary of Honeywell International, Inc., for the U.S. Department of Energy's National Nuclear Security Administration under contract DE-NA-0003525.

References

[1] Poludnenko, A.Y. and Oran, E.S., "The interaction of high-speed turbulence with flames: Turbulent flame speed", *Combustion and Flame* (2011) 301-326.

[2] Peters, N., *Turbulent Combustion*, Cambridge University Press (2000).

[3] Skiba, A.W., Wabel, T.M., Carter, C.D., Hammack, S.D., Temme, J.E., and Driscoll, J.F., "Premixed flames subjected to extreme levels of turbulence part 1: Flame structure and a new measured regime diagram", *Combustion and Flame* 189 (2018) 407-432.

[4] Aspden, A.J., Day, M.S., and Bell, J.B., "Turbulence-flame interactions in lean premixed hydrogen: transition to the distributed burning regime", *Journal of Fluid Mechanics* 680 **(**2011) 287-320.

[5] Chen, Y.-C., Peters, N., Schneemann, G.A., Wruck, N., Renz, U., and Mansour, M.S., "The detailed flame structure of highly stretched turbulent premixed methane-air flames", *Combustion and Flame* 107 **(**1996) 223-244.

[6] Mansour, M.S. and Chen, Y.-C., "Highly strained turbulent rich methane flames stabilized by hot combustion products", *Combustion and Flame* 116 **(**1999) 136-153.

[7] Dunn, M.J., Masri, A.R., and Bilger, R.W., "A new piloted premixed jet burner to study strong finite-rate chemistry effects", *Combustion and Flame* 151 (2007) 46-60.

[8] Dunn, M.J., Masri, A.R., Bilger, R.W., Barlow, R.S., and Wang, G.H., "The compositional structure of highly turbulent piloted premixed flames issuing into a hot coflow", *Proceedings of the Combustion Institute* 32 (2009) 1779-1786.

[9] Dunn, M.J., Masri, A.R., Bilger, R.W., and Barlow, R.S., "Finite rate chemistry effects in highly sheared turbulent premixed flames", *Flow, Turbulence and Combustion* (1998) 759-766.

[10] Zhou, B., Brackmann, C., Li, Q., Wang, Z, Petersson, P., Li, Z., Alden, M., and Bai, X.S., "Distributed reactions in highly turbulent premixed methane/air flames Part 1. Flame structure characterization", *Combustion and Flame* 162 (2015) 2937-2953.

[11] Wang, H., Hawkes, E.R., Savard, B., and Chen, J.H., "Direct numerical simulation of a high Ka CH_4/air stratified premixed jet flame", *Combustion and Flame* 193 (2018) 229-245.

[12] Wabel, T.M., Skiba, A.W., Temme, J.E., and Driscoll, J.F., "Measurements to determine the regimes of premixed flames in extreme turbulence", *Proceedings of the Combustion Institute* 36 (2017) 1809-1816.

[13] Wabel, T.M., Skiba, A.W., and Driscoll, J.F., "Turbulent burning velocity measurements: Extended to extreme levels of turbulence", *Proceedings of the Combustion Institute* 36 (2017) 1801-1808.

[14] Osborne, J.R., Ramji, S.A., Carter, C.D., and Steinberg, A.M., "Relationship between local reaction rate and flame structure in turbulent premixed flames from simultaneous 10 kHz TPIV, OH PLIF, and CH_2O PLIF", *Proceedings of the Combustion Institute* 36 (2017) 1835-1841.

[15] Fuest, F., Barlow, R.S., Geyer, D., Seffrin, F., and Dreizler, A., "A hybrid method for data evaluation in 1-D Raman spectroscopy", *Proceedings of the Combustion Institute* 33 (2011) 815-822.

[16] Driscoll, J.F., "Turbulent premixed combustion: Flamelet structure and its effect on turbulent burning velocity", *Progress in Energy and Combustion Science* 34 (2008) 91-134.

[17] Magnotti, G., Geyer, D., and Barlow, R.S., "Interference free spontaneous Raman spectroscopy for measurements in rich hydrocarbon flames", *Proceedings of the Combustion Institute* 35 (2015) 3765-3772.

[18] Sweeney, M.S., Hochgreb, S., Dunn, M.J., and Barlow, R.S., "Multiply conditioned analyses of stratification in highly swirling methane/air flames", *Combustion and Flame* 160 (2013) 322-334.

[19] Sweeney, M.S., Hochgreb, S., Dunn, M.J., and Barlow, R.S., "The structure of turbulent stratified and premixed methane/air flames I: Non-swirling flows", *Combustion and Flame* 159 (2012) 2896-2911.

[20] Bilger, R.W., Starner, S.H., and Kee, R.J., "On reduced mechanisms for methane-air combustion in nonpremixed flames", *Combustion and Flame* 80 (1990) 135-149.

[21] Barlow, R.S., Dunn, M.J., Sweeney, M.S., and Hochgreb, S., "Effects of preferential transport in turbulent bluff-body-stabilized lean premixed CH4/air flames", *Combustion and Flame* 159 (2012) 2563-2575.

[22] Barlow, R.S., Magnotti, G., Cutcher, H.C., and Masri, A.R., "On defining progress variable for Raman/Rayleigh experiments in partially-premixed methane flames", *Combustion and Flame* 179 (2017) 117-129.

[23] Najm, H.N., Paul, P.H., Mueller, C.J., and Wyckoff, P.S., "On the adequacy of certain experimental observables as measurements of flame burning rate", *Combustion and Flame* 113 (1998) 312-332.

[24] Peters, N. and Williams, F.A., "The asymptotic structure of stoichiometric methane-air flames", *Combustion and Flame* 68 (1987) 185-207.

[25] Frank, J.H. and Barlow, R.S., "Simultaneous Rayleigh, Raman, and LIF measurements in turbulent premixed methane-air flames", *27th Symposium (International) on Combustion* (1998) 759-766.